

ACCEPTED MANUSCRIPT

## Influence of typical technological parameters on the processing quality of laser surface texturing technology for finger sealing

To cite this article before publication: Lingping Chen *et al* 2024 *Surf. Topogr.: Metrol. Prop.* in press <https://doi.org/10.1088/2051-672X/ad993e>

### Manuscript version: Accepted Manuscript

Accepted Manuscript is “the version of the article accepted for publication including all changes made as a result of the peer review process, and which may also include the addition to the article by IOP Publishing of a header, an article ID, a cover sheet and/or an ‘Accepted Manuscript’ watermark, but excluding any other editing, typesetting or other changes made by IOP Publishing and/or its licensors”

This Accepted Manuscript is © 2024 IOP Publishing Ltd. All rights, including for text and data mining, AI training, and similar technologies, are reserved..



During the embargo period (the 12 month period from the publication of the Version of Record of this article), the Accepted Manuscript is fully protected by copyright and cannot be reused or reposted elsewhere.

As the Version of Record of this article is going to be / has been published on a subscription basis, this Accepted Manuscript will be available for reuse under a CC BY-NC-ND 3.0 licence after the 12 month embargo period.

After the embargo period, everyone is permitted to use copy and redistribute this article for non-commercial purposes only, provided that they adhere to all the terms of the licence <https://creativecommons.org/licenses/by-nc-nd/3.0>

Although reasonable endeavours have been taken to obtain all necessary permissions from third parties to include their copyrighted content within this article, their full citation and copyright line may not be present in this Accepted Manuscript version. Before using any content from this article, please refer to the Version of Record on IOPscience once published for full citation and copyright details, as permissions may be required. All third party content is fully copyright protected, unless specifically stated otherwise in the figure caption in the Version of Record.

View the [article online](#) for updates and enhancements.

# Influence of Typical Technological Parameters on the Processing Quality of Laser Surface Texturing Technology for Finger Sealing

Lingping Chen<sup>1,2</sup>, Yanchao Zhang<sup>2\*</sup>, Guoqiang Chen<sup>1</sup>, Jiewei Li<sup>1</sup>, Bowei Zhang<sup>1</sup>, and Mingfeng Wang<sup>3</sup>

1. School of Mechanical Engineering, Hunan Institute of Engineering, Xiangtan, Hunan, 411104, China

2. School of Mechanical and Precision Instrumental Engineering, Xi'an University of Technology, Xi'an, 710048, China

3. Department of Mechanical and Aerospace Engineering, Brunel University London, London, UB8 3PN, United Kingdom

\* Corresponding author: Yanchao Zhang, School of Mechanical and Precision Instrumental Engineering, Xi'an University of Technology, No. 5 Jinhua South Road, Beilin District, Xi'an, Shaanxi 710048, China; Email: zhangyanchao@xaut.edu.cn; Tel.: +86-135-7187-4962

**Abstract:** In recent years, to achieve favorable tribological characteristics, surface texture technology for friction reduction has been extensively studied, and its effectiveness has been successfully validated. The quality of surface texture processing directly impacts the tribological performance of finger seal friction pairs. To investigate the influence of the laser process parameters on the finger seal surface texture of the GH4169 and improve its processability and process predictability, a comparative experiment and analysis involving multiple processing parameters, including the laser power ( $P$ ), laser frequency ( $F$ ), scanning speed ( $V$ ), and scanning times ( $N$ ), were conducted. To evaluate the quality of laser surface texturing processing technology, four processing morphology parameters were established. Uniform experiments and regression analysis were employed to analyze the influence and synergistic effects of laser processing parameters on processing quality. The research results indicate that laser power, scanning times, and scanning speed are the main process parameters that significantly affect laser surface deformation. The outer diameter is directly proportional to the laser power and inversely proportional to the scanning speed; the bottom diameter ratio is directly proportional to both the laser power and scanning times; and the pit depth initially increases and then decreases with increasing laser power and scanning times. The suitable range of processing parameters is as follows: laser power (10~20%), speed range (400~700 mm/s), scanning times (8~18 times), and laser frequency (20~25 kHz). This research provides theoretical and experimental support for the precise control of surface texture prepared by laser processing of GH4169, laying the foundation for friction and wear tests of textured finger seals.

**Keywords:** Laser surface texturing; Process parameters; Surface topography; Finger seal; GH4169

## 1. Introduction

As a new type of flexible seal developed after brush seals, finger seals have the potential for low leakage rates, long service life, and high cost-effectiveness<sup>[1]</sup>. The direct contact between the finger feet and the rotor inevitably produces friction and wear, so the wear performance between them becomes an important factor affecting the working stability of finger seals<sup>[2]</sup>. At present, methods to improve the wear resistance of finger seals mainly include new materials<sup>[3]</sup>, new structures<sup>[4]</sup>, and surface coatings<sup>[5]</sup>. However, these methods have not yet achieved the ideal effect of wear and friction reduction of finger

1  
2  
3 seals, in other words, there is a gap in further exploration of other methods.

4  
5 Recently, numerous studies have shown that using surface texture to improve the tribological  
6 performance of friction pairs is one of the most successful engineering applications<sup>[6,7]</sup>. The potential  
7 mechanisms by which surface texture improves friction and wear properties can be explained as micro  
8 hydrodynamic bearing, inlet suction, oil reservoir, and debris trapping effects<sup>[8,9]</sup>. Wang et al.<sup>[10]</sup> proposed  
9 a new type of "pocket-textured surface" and carried out tribological experiments and finite element  
10 analysis. The results show that the surface texture can improve the tribological properties of line contacts  
11 under extremely unlubricated conditions, and the friction coefficient is 48% lower than that of  
12 nontextured surfaces. Zhou et al.<sup>[11]</sup> machined several kinds of array textures (square, circular, elliptical,  
13 and rhombic) on the interference fit surface and studied the effect of texture parameters on the  
14 interference fit disassembly damage reduction through disassembly experiments. The results show that  
15 the effect of the texture equivalent circle diameter on disassembly damage is the greatest, followed by  
16 the texture shape and surface density. In addition, the load-carrying capacity test revealed that the load-  
17 carrying capacity of the surface with excellent texture increased by approximately 40%.  
18 Velayuthaperumal et al.<sup>[12]</sup> fabricated dimple, moat, and hybrid surface textures on the surface of a  
19 Ti6Al4V alloy. The surface properties, such as microhardness, wettability, friction, wear, and elemental  
20 analysis, were studied via wear tests. The results show that the tribological properties of the textured  
21 surface are better than those of the nontextured surface. Moreover, the moat texture is more effective for  
22 the functional surface formation of Ti6Al4V biomaterials, followed by the hybrid and dimple structures.

23  
24 Motivated by surface textures effectively improving the tribological properties of the friction  
25 interface, the authors have also attempted to improve the tribological characteristics of finger seals via  
26 surface texture technology<sup>[13,14]</sup>. Based on several common surface texture forms (such as diamond,  
27 hexagonal, circular, and triangular), numerical analysis methods have been used to study the influence  
28 of the geometric parameters of surface textures and working conditions on the performance of textured  
29 finger seals. Research results show that adding surface textures can effectively enhance the  
30 hydrodynamic capacity between the friction pairs of finger seals, helping to lift the finger feet and avoid  
31 friction and wear caused by direct contact with the friction pairs. However, under actual working  
32 conditions, finger seals are subject to complex effects such as fluid flow, structural vibration, heat transfer,  
33 and friction wear, which pose significant challenges to the accuracy, efficiency, and reliability of  
34 numerical simulation studies. Therefore, it is necessary to conduct experimental research on the  
35 performance of textured finger seals.

36  
37 The quality of surface texture processing directly affects the tribological performance of friction  
38 pairs and is crucial for experimental research on finger seals. Currently, many typical processing  
39 technologies have been applied to the preparation of surface textures, such as laser processing<sup>[15,16]</sup>,  
40 electrical discharge machining<sup>[17,18]</sup>, electrochemical machining<sup>[19,20]</sup>, and abrasive jet processing<sup>[21]</sup>. The  
41 applicable scopes, advantages, and disadvantages of various processing technologies are shown in  
42 Appendix Table A1. Among them, laser surface texturing (LST) is the most widely used method because  
43 of its high processing efficiency, wide range of applicable materials, and environmental friendliness<sup>[22]</sup>.  
44 Considering the materials of the test samples and the test conditions of the research group, this study  
45 chooses LST technology to prepare surface textures. In the LST process, in addition to the selection of  
46 laser types, the surface morphology and feature sizes can be controlled by adjusting the laser processing  
47 parameters, such as the laser power intensity, laser spot size, and pulse repetition frequency. Li et al.<sup>[23]</sup>  
48 investigated the influence of laser processing parameters on the surface texture of polyformaldehyde  
49 (POM). Several machining parameters, such as the laser power, scanning speed, and pulse width, were  
50  
51  
52  
53  
54  
55  
56  
57  
58  
59  
60

1  
2  
3 compared and analyzed. The experimental results show that the laser power and scanning speed  
4 significantly affect the texture depth. A higher laser power and lower scanning speed are favorable for  
5 increasing the depth of formation. The surface roughness at the bottom of the texture increases with  
6 increasing scanning speed and first increases but then decreases with increasing laser power. Yang et  
7 al.<sup>[24]</sup> investigated the effect of the number of pulses on the ablation characteristics of bearing steel GCr15  
8 as processed by the LST. As the pulse number increased from 10 to 90, the radius of the texture feature  
9 increased from 12.72 to 13.37  $\mu\text{m}$ . Ahuir-Torres et al.<sup>[25]</sup> compared the surface morphology of Ti6Al4V  
10 alloys treated with nanosecond and picosecond laser ablation LSTs. Compared with a nanosecond laser,  
11 the application of a picosecond laser can significantly reduce the heat-affected zone. Moreover, in the  
12 process of laser ablation, a short pulse duration can reduce the undesirable thermal effect and improve  
13 the precision of the microstructure.  
14

15  
16  
17 The above literature has a certain reference value for selecting process parameters and determining  
18 the process quality of LST technology to prepare surface textures in this paper. However, most of the  
19 literature adopts single-factor analysis methods, which analyze the impact of one process parameter on  
20 processing quality at a time. This method requires many experiments, which is time-consuming and  
21 labor-intensive. Moreover, the obtained analysis results may be unreliable due to the neglect of the  
22 interaction between process parameters. Additionally, the processing parameters of the surface texture  
23 are related to the material being processed. Therefore, it is necessary to research the processing  
24 technology of surface textures for finger seals and study the influence of laser processing parameters on  
25 the quality of surface texture processing to optimize the processing parameters. This lays the foundation  
26 for subsequent friction and wear tests of textured finger seal pin-discs and even bench performance tests.  
27

28  
29 The structure of this paper is as follows: In Section 2, the materials and methods are introduced, the  
30 design of experiments (DOE) and data statistical analysis methods are determined, and four processing  
31 morphology parameters (such as the outer diameter ( $D$ ), pit bottom diameter ( $D_t$ ), pit depth ( $H$ ), and  
32 depth fluctuation height ( $H_f$ )) are formulated to evaluate the processing quality. In Section 3, the results  
33 are analyzed. Statistical analysis is used to carry out regression analysis on the four processing  
34 morphology parameters, obtaining the influence of the laser processing parameters on the processing  
35 quality and the synergistic effects of each parameter on the processing quality. Section 4 presents the  
36 conclusion and discussion.  
37

## 38 39 40 41 42 **2. Materials and methods**

### 43 44 45 **2.1 Processing materials**

46  
47 Commonly used materials for finger seal friction pairs include the cobalt-based superalloy GH605  
48 and the nickel-based superalloy GH4169. Among them, GH4169, which is used as the rotor material,  
49 exhibits excellent comprehensive performance within the temperature range of -253 to 650  $^{\circ}\text{C}$  (i.e., it  
50 demonstrates superior fatigue resistance, radiation resistance, oxidation resistance, corrosion resistance,  
51 and machinability). The yield strength of GH4169 below 650  $^{\circ}\text{C}$  ranks first among wrought superalloys.  
52 Since finger laminates are extremely thin, surface texturing is performed on the circumferential surface  
53 of the rotor. Therefore, GH4169 is prepared as a disk sample with a diameter of 30 mm and a height of  
54 5 mm, as shown in Figure 1.  
55  
56  
57  
58  
59  
60



**Figure 1. Test piece.**

A Huatuo LR-Fib-30T fiber laser marking machine was used for texture processing. Its specific parameters are listed in Table 1.

**Table 1. Parameters of the Huatuo LR-Fib-30T optical fiber laser marking machine**

Scanning speed (mm/s)	Laser frequency (KHz)	Repetition accuracy (mm)	Pulse width (ns)	Output power (W)	Power adjustment range	Laser wavelength (nm)
≤8,000	20~200	±0.003	100	60	1~100%	1064

The disk samples are fabricated through laser cutting of GH4169 plates, resulting in a surface quality that is not optimal. Therefore, surface grinding and polishing are necessary before processing the surface texture. Additionally, during the LST, owing to the high instantaneous laser energy, ablation, and slag phenomena occur around the texture, increasing the surface roughness and significantly affecting the friction and wear performance. Consequently, after the LST is completed, further grinding and polishing are required to ensure the desired surface quality. After grinding and polishing, ultrasonic cleaning of the sample is necessary to ensure that the surface texture of the micropits has good morphological characteristics and application effects. The surface morphology measurement equipment used in the experiment was a laser confocal scanning microscope (LEXT-OLS4000). Figure 2 shows the surface morphology of the disk sample after polishing and cleaning. The figure shows that the sample surface is smooth and flat, and the average roughness  $R_a$  is 1.66 nm.

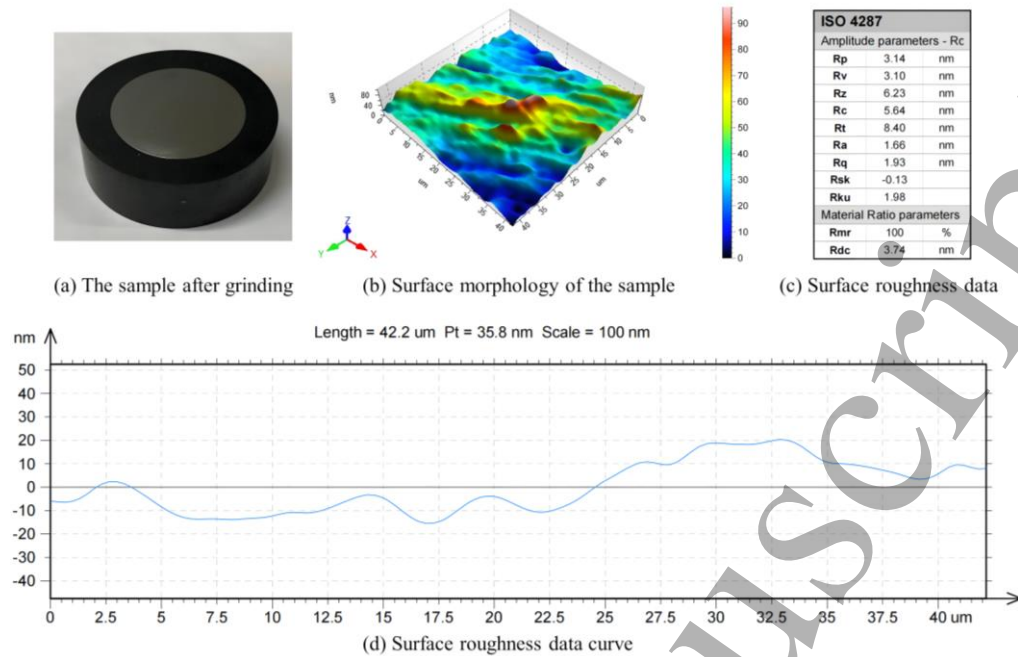


Figure 2. Surface morphology of the sample after polishing and cleaning

## 2.2 Design of experiments

LST is a crucial step in the experimental study of finger sealing performance, and the correct selection of laser processing parameters plays a decisive role in the processing quality of surface texture. Research has indicated that many technological parameters affect the quality of laser processing, such as the laser power, laser frequency, scanning speed, scanning times, spot diameter, and negative defocusing amount, and that each parameter has a wide range of adjustments. To reduce the number of experiments and quickly identify the influence of laser processing parameters on processing quality, design of experiments (DOE) is employed to design processing experiments. For experiments with multiple factors and levels, commonly used DOE methods include orthogonal experimental design and uniform experimental design. Compared with the orthogonal experimental design, the uniform experimental design distributes the design points evenly in the experimental range, obtains more information with fewer experimental points, and has the advantages of "uniform distribution" and fewer experimental times. Therefore, a uniform experimental design is adopted in this paper.

This paper mainly analyses four factors that have the greatest impact on laser processing quality, namely, laser power ( $P$ ), laser frequency ( $F$ ), scanning speed ( $V$ ), and scanning times ( $N$ ). Notably, the pulse width is a critical factor in determining the processing characteristics<sup>[26]</sup>, but the pulse width of the laser marking machine used in this paper is not adjustable, and the factory setting is 100 ns. According to the results of preliminary experiments, excessive power, too many scanning times, and too low of a scanning speed cause severe burning. Therefore, each parameter is set to 10 levels, as shown in Table 2.

The total laser power is 60 W, and the laser power value in the experiment is the percentage of power.

**Table 2. Parameter setting of the processing technology test**

Level	Laser power ( $P/\%$ )	Scanning speed ( $V/\text{mm/s}$ )	Laser frequency ( $F/\text{KHz}$ )	Scanning times ( $N/\text{times}$ )
1	5	100	20	2
2	10	200	25	4
3	15	300	30	6
4	20	400	35	8
5	25	500	40	10
6	30	600	45	12
7	35	700	50	14
8	40	800	55	16
9	45	900	60	18
10	50	1,000	65	20

The DPS (Data Processing System, version 9.5, Zhejiang University) data processing system was used for the experimental design. This software is currently the most popular multifunctional statistical analysis software in China, with complete experimental design and statistical analysis functions. DPS has outstanding performance in constructing large-scale uniform-design tables and mixed-design tables. This experiment has a total of 4 experimental factors, and each factor is set to 10 levels. The number of experiments is set to 4 times the number of levels (i.e., 40), which is conducive to data modeling and optimization, with a maximum number of iterations of 1,000 and time control within 5 minutes, and a uniform experimental table is designed. According to the author's previous research<sup>[13,14]</sup>, in finger sealing applications, circular and hexagonal textures have better friction and wear resistance than triangular, diamond, and rectangular textures. In addition, since the hexagon has six vertices, it is convenient to connect the diagonal vertices to measure the outer circle diameter after machining. Thus, a series of hexagonal textures with an outer diameter of 400  $\mu\text{m}$  were processed on the GH4169 disc.

### 2.3 Data statistical analysis methods

After the LST was completed, the morphological characteristics of the hexagonal texture were measured via a confocal interference microscope. To evaluate processing quality, four morphological parameters were established: the outer diameter ( $D$ ), pit bottom diameter ( $D_i$ ), pit depth ( $H$ ), and depth fluctuation height ( $H_f$ ), as shown in Figure 3. The outer diameter was measured along three diagonals and averaged, and the pit depth, bottom diameter, and depth fluctuation height were measured along three diagonal sections and horizontal sections and were averaged. The measurement results are shown in Table 3.

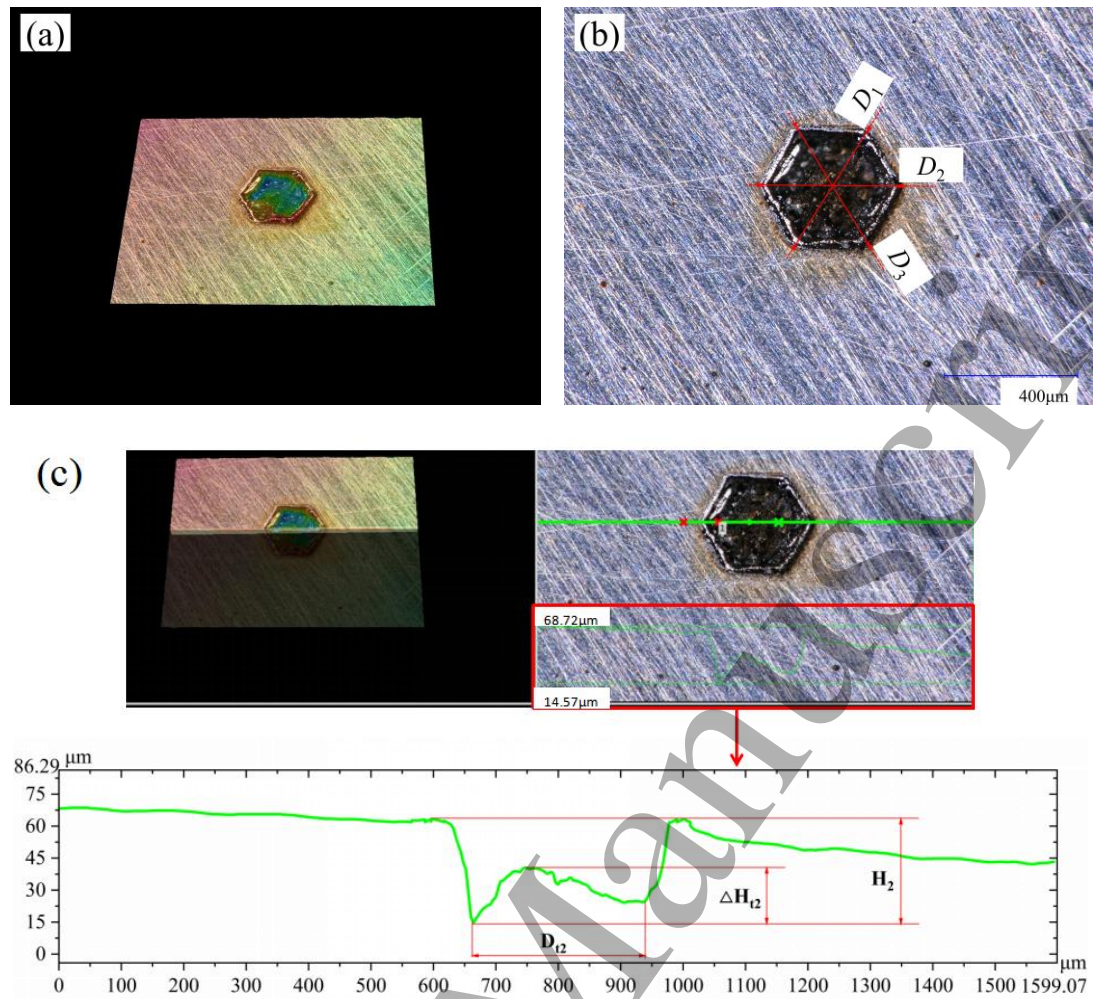


Figure 3. Texture processing morphology: (a) three-dimensional overall morphology; (b) circumcircle diameter; (c) pit depth, bottom diameter, and depth fluctuation

Table 3. Uniformity test table and measurement results of topography characteristics after laser processing

Test No.	Laser power (P/%)	Scanning speed (V/mm/s)	Laser frequency (F/KHz)	Scanning times (N/times)	Outer diameter (D/μm)	Bottom diameter (D <sub>t</sub> /μm)	Pit depth (H/μm)	Depth fluctuation (H <sub>t</sub> / μm)
N1	10	1,000	45	12	409.00	238.33	103	70
N2	15	300	65	2	421.67	179.67	93.25	69
N3	25	700	60	10	428.00	308.67	76.5	58.5
N4	5	800	65	14	390.67	185.00	58.25	63.25
N5	5	100	35	8	435.67	314.33	64	50.75
N6	45	100	50	20	515.33	377.67	28.25	34
N7	35	200	40	10	460.33	361.67	25.5	22.5
N8	50	200	25	4	448.00	364.67	29.5	25.75

Test No.	Laser power (P/%)	Scanning speed (V/mm/s)	Laser frequency (F/KHz)	Scanning times (N/times)	Outer diameter (D/μm)	Bottom diameter (D <sub>t</sub> /μm)	Pit depth (H/μm)	Depth fluctuation (H <sub>t</sub> /μm)
N9	40	800	30	16	430.67	342.67	36	25.5
N10	35	600	20	20	427.67	342.00	32	25.5
N11	50	1,000	40	18	434.33	355.00	42	31
N12	25	400	40	20	439.67	353.00	40.5	32.25
N13	10	600	40	4	420.67	201.00	79.25	56.75
N14	30	100	25	12	438.00	360.33	44.5	36.25
N15	15	300	30	18	418.67	342.67	44.25	26.5
N16	20	1,000	25	8	403.00	246.67	62.75	44.25
N17	20	500	35	16	414.00	326.33	42	30
N18	5	700	25	18	384.00	243.67	34.75	51.75
N19	5	500	50	4	399.67	262.67	47.25	51.75
N20	20	700	50	12	406.33	329.67	42	27
N21	30	400	45	2	444.00	220.00	40.75	43.75
N22	45	700	35	2	452.67	244.67	31.25	41.75
N23	50	400	65	12	451.00	341.33	61.5	40
N24	15	800	30	6	390.00	216.67	70.75	72.75
N25	40	300	30	6	410.00	267.67	52.75	48.5
N26	40	300	55	16	452.00	347.00	30	33
N27	25	200	45	14	431.67	366.67	23.5	31.25
N28	20	100	55	6	455.33	351.33	43	28.5
N29	30	600	65	18	413.33	328.33	43.25	36.5
N30	15	900	55	20	402.33	310.67	31.25	23.5
N31	10	400	20	10	390.67	245.67	36.25	45.5
N32	40	800	50	10	412.00	345.67	21.5	29.25
N33	35	1,000	55	4	391.67	252.33	34.25	27.5
N34	45	900	60	6	406.00	319.00	44.5	36.25
N35	35	500	60	8	427.33	349.33	35	29.5
N36	10	200	60	16	426.00	344.33	25.5	27.5
N37	30	900	35	14	411.67	329.67	30.5	34.5
N38	50	600	45	8	436.00	354.00	35	29.5
N39	45	500	20	14	443.67	350.00	37	33.5
N40	25	900	20	2	405.00	229.67	41.25	47

Using the Statistical Product and Service Solutions (SPSS) system, regression analysis was performed on the measurement results in Table 3 to determine the impact of the processing parameters on the four morphological characteristics and to obtain relevant processing rules, allowing for the optimization of the best processing parameter combination.

### 3. Results and discussion

#### 3.1 Regression analysis of the outer diameter

Since there are four processing parameters, this analysis involves multiple independent variables affecting a single dependent variable. Therefore, multiple linear regression was chosen. Table 4 shows the regression model summary, where the R-squared value is 66.4%, indicating that 66.4% of the variation in the outer diameter is due to the four independent variables considered in this analysis, suggesting that the regression model is relatively accurate and that the statistical model is successful.

**Table 4. Summary of multivariate linear regression models of outer diameter**

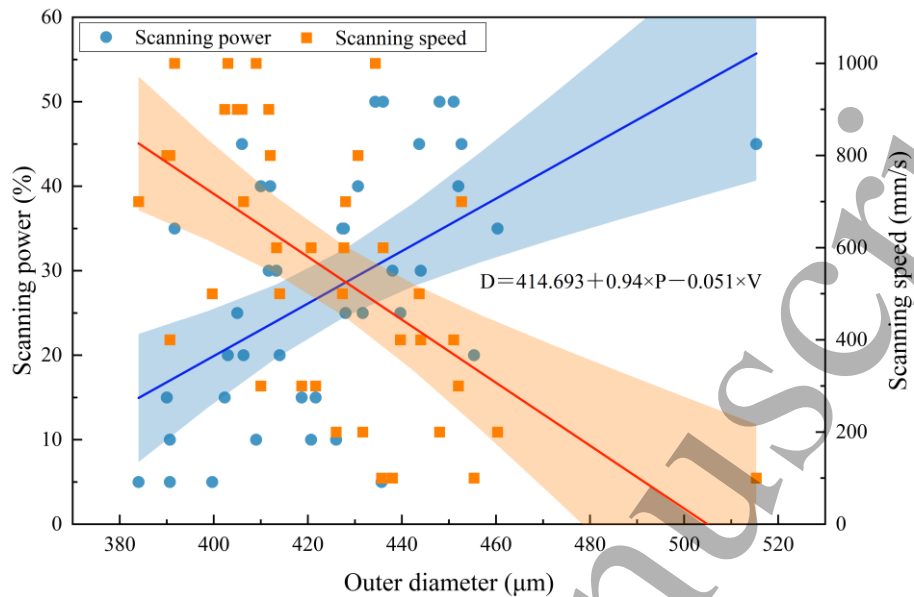
R	R square	Adjusted R square	Standard error of the estimate	Durbin-Watson (U)
.815 <sup>a</sup>	.664	.626	15.42859	1.577

Table 5 presents the regression coefficients, in which the significance level statistically demonstrates the correlation between the independent variables and the dependent variable. This reflects that the laser power and scanning speed have significant impacts on the outer diameter (significance level < 0.05), whereas the laser frequency and scanning times have little influence on the outer diameter. Furthermore, the regression coefficient corresponding to the laser power is positive, indicating that the larger the laser power is, the greater the outer diameter. Conversely, the regression coefficient of the scanning speed becomes negative, suggesting that the higher the scanning speed is, the smaller the outer diameter. Based on the absolute values of the standardized coefficients, the scanning speed has the greatest impact on the outer diameter, followed by the laser power.

**Table 5. Multiple linear regression coefficients of the outer diameter**

Model	Unstandardized coefficients		Standard coefficients	t	Significance	Collinearity statistics	
	B	Standard error	Beta			Tolerance	VIF
(Constant)	414.693	11.248		36.869	.000		
Laser power ( <i>P</i> )	.940	.170	.542	5.532	.000	1.000	1.000
Scanning speed ( <i>V</i> )	-.051	.008	-.591	-6.030	.000	1.000	1.000
Laser frequency ( <i>F</i> )	.150	.170	.086	.881	.384	1.000	1.000
Scanning times ( <i>N</i> )	.520	.425	.120	1.223	.229	.999	1.001

From the coefficient table, the quantitative relationship between the outer diameter and process parameters can be fitted as:  $D = 414.693 + 0.94 \times P - 0.051 \times V$ . The data statistics and fitting are shown in Figure 4.



**Figure 4. Data statistics and fitting of the outer diameter**

To verify the reliability of this regression model, three diagnostics were performed: ① Multicollinearity check: The linear regression model requires that there is no multicollinearity among the independent variables. When the variance inflation factor (VIF) in the coefficient table is less than 5, there is no multicollinearity among the independent variables. In this regression model, the VIF values for all four independent variables are less than 5, meeting the requirement. ② Normality of residuals: The residuals of the data should follow a normal distribution. The normal P–P plot of the regression model (as shown in Figure 5) indicates that the residuals' scatter points fall on or near the diagonal line, satisfying the normal distribution requirement. ③ Independence of residuals: There should be no serial correlation among the samples. This can be judged by the Durbin–Watson (D–W) value in the model summary. A D–W value close to 2 indicates no serial correlation among variables. The D–W value for this regression model is 1.577. Additionally, since the sample data in this regression model is cross-sectional data rather than time series data, serial correlation can be disregarded.

All three diagnostic requirements are met, confirming that the relationship between the outer diameter and process parameters established by this regression model is stable and reliable.

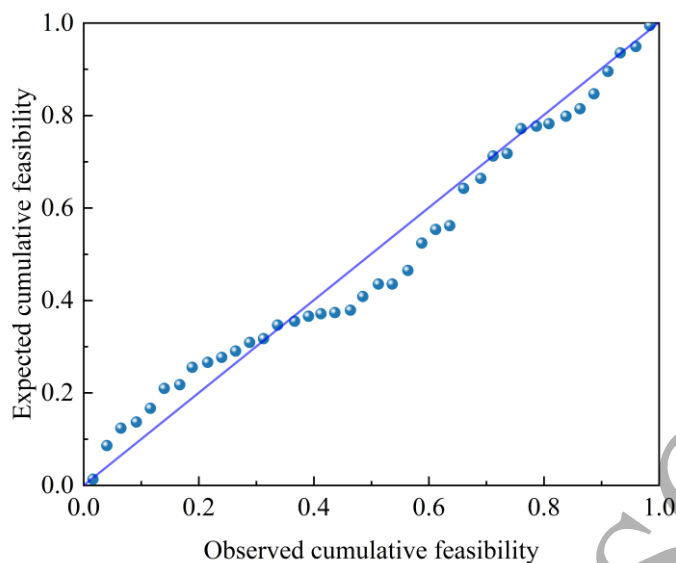


**Figure 5. Normalized residual P–P diagram for regression analysis of the outer diameter**

### 3.2 Regression analysis of the bottom diameter ratio

The larger the bottom diameter is, the flatter the bottom of the pit. The bottom diameter ratio  $\Delta D$  (the ratio of the bottom diameter to the outer diameter) is used for analysis. Like the regression analysis of the outer diameter, multiple linear regression is used to statistically analyze the factors affecting the bottom diameter ratio. Table 6 shows the regression model summary, where the R-squared value is 52.2%, indicating that the regression model is relatively accurate and that the statistical model is successful.

**Table 6. Summary of the multivariate linear regression model for the bottom diameter ratio**

R	R square	Adjusted R square	Standard error of the estimate	Durbin-Watson (U)
.722 <sup>a</sup>	.522	.467	8.74171	1.921

Table 7 shows the regression coefficients. The table shows that the independent variables that significantly affect the bottom diameter ratio are the laser power, and scanning times (significance < 0.05), whereas the laser frequency and scanning times have little effect on the bottom diameter ratio. In addition, the regression coefficients of both the laser power and scanning times are positive, indicating that the greater the laser power and scanning times are, the greater the bottom diameter ratio, that is, the smoother the morphology of the processed micro pit. According to the absolute value of the standardized coefficient, the scanning times have the greatest impact on the proportion of the bottom diameter, followed by the laser power.

**Table 7. Multiple linear regression coefficients of the bottom diameter rate**

Model	Unstandardized coefficients		Standard coefficients	t	Significance	Collinearity statistics	
	B	Standard error	Beta			Tolerance	VIF
(Constant)	54.053	6.373		8.482	.000		
Laser power ( $P$ )	.350	.096	.425	3.639	.001	1.000	1.000
Scanning Speed ( $V$ )	-.009	.005	-.209	-1.787	.083	1.000	1.000
Laser Frequency ( $F$ )	.002	.096	.003	.023	.982	1.000	1.000
Scanning times ( $N$ )	1.119	.241	.544	4.651	.000	.999	1.001

From the coefficient table, the quantitative relationship between the bottom diameter ratio and process parameters can be fitted as  $\Delta D = 54.053 + 0.35 \times P + 1.119 \times N$ . The data statistics and fitting are shown in Figure 6. The reliability diagnostics for this regression model are similar to those for the outer diameter analysis and are not repeated here.

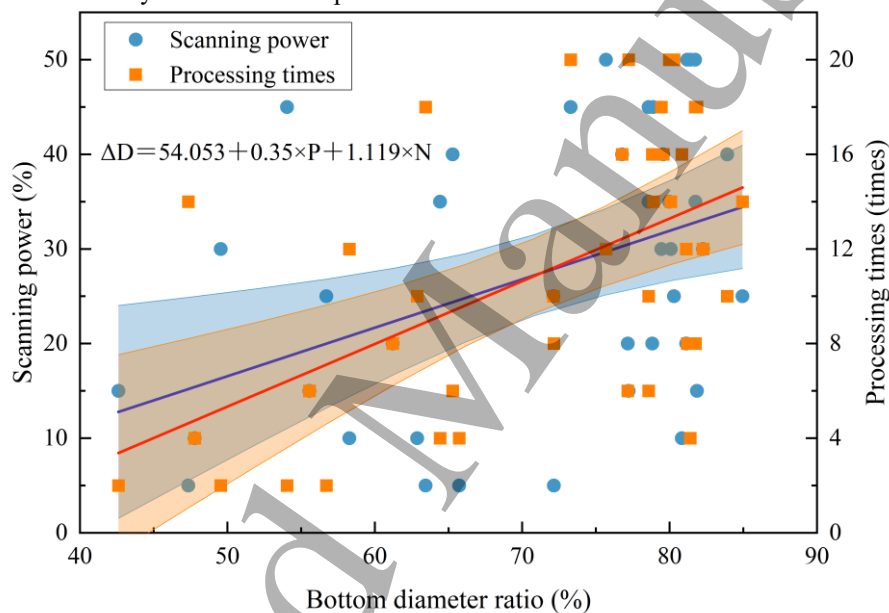


Figure 6. Data statistics and fitting of the bottom diameter ratio

### 3.3 Regression analysis of pit depth

Before performing regression analysis on pit depth, a correlation analysis between pit depth and processing parameters was conducted, as shown in Table 8. The correlation analysis shows that pit depth is negatively correlated with laser power and scanning times, which contradicts the usual experience that higher laser power and more scanning times result in deeper processing. Therefore, a simple linear model cannot be used for regression; instead, a multivariate nonlinear regression model should be used. The initial assumption is:  $H = a + b \times P + c \times N + d \times P^2 + e \times N^2 + f \times P \times N$ .

Table 8. Correlation analysis of pit depth and processing parameters

Correlation		Laser power ( $P$ )	Scanning speed ( $V$ )	Laser frequency ( $F$ )	Scanning times ( $N$ )
Pit depth ( $H$ )	Pearson correlation	-.413**	.174	.155	-.303*
	Significance (Two-tailed)	.008	.283	.339	.047

\*\*Indicates that the correlation is significant at a confidence level (two-tailed) of 0.01.

\*Indicates that the correlation is significant at a confidence level (two-tailed) of 0.05.

Table 9 shows the multivariate nonlinear regression parameters of the pit depth. The regression equation for pit depth can be fitted as  $H = 90.374 - 1.831 \times P - 1.429 \times N + 0.011 \times P^2 - 0.062 \times N^2 + 0.066 \times P \times N$ . To verify the accuracy of this regression model, partial derivatives concerning the laser power ( $P$ ) and scanning times ( $N$ ) were taken, and the resulting system of linear equations was solved to obtain  $P = 45.3639$  and  $N = 12.6211$ . This indicates that when the laser power is 45% and the number of scanning times is 12, the pit depth is minimized, with a value of 39.82  $\mu\text{m}$ .

**Table 9. Multivariate nonlinear regression parameters of pit depth**

Parameter	Estimate	Standard error	95% Confidence interval	
			Lower bound	Upper bound
a	90.374	8.495	73.593	107.155
b	-1.831	.450	-2.719	-.943
c	-1.429	1.107	-3.617	.758
d	.011	.007	-.004	.025
e	-.062	.045	-.152	.027
f	.066	.016	.033	.098

Moreover, a 2D contour map was plotted with the measured data of pit depth, laser power, and scanning times, as shown in Figure 7. The figure shows the following: ① The minimum pit depth corresponds to a laser power of 40% and 10 scanning times, matching the results from the multivariate nonlinear regression model and confirming its reliability; ② As the laser power increases, the pit depth first increases and then decreases, and the pit depth is relatively large when the laser power ranges from 10% to 20%. This occurs because as the laser power increases, the laser energy also increases, which accelerates the speed of melting/evaporation, thus gradually increasing the pit depth. However, as the laser power continues to increase, the large thermal effect leads to an increase in the temperature gradient, and the Marangoni effect<sup>[27]</sup> is enhanced and coupled with recoil pressure<sup>[27]</sup> to drive the melt to flow along the solid-liquid line to the bottom of the melt pool and stack up<sup>[28,29]</sup>. Besides, plasma gradually formed above the molten pool during the vaporization, plasma shielding effect<sup>[30]</sup> will affect the laser energy

conduction to a certain extent, so the processing depth decreases. ③ As the scanning times increase, the pit depth also tends to first increase and then decrease, and the pit depth is relatively large when the scanning times range from 8 to 14. This is because as the scanning times increase, the pit depth gradually increases. However, with increasing scanning times and processing depth, owing to the increase of the defocus amount<sup>[31]</sup> and plasma shielding effect<sup>[32]</sup>, the energy density near the laser focus decreases, and the exclusion effect of the melt becomes worse, resulting in a decreasing trend in depth.

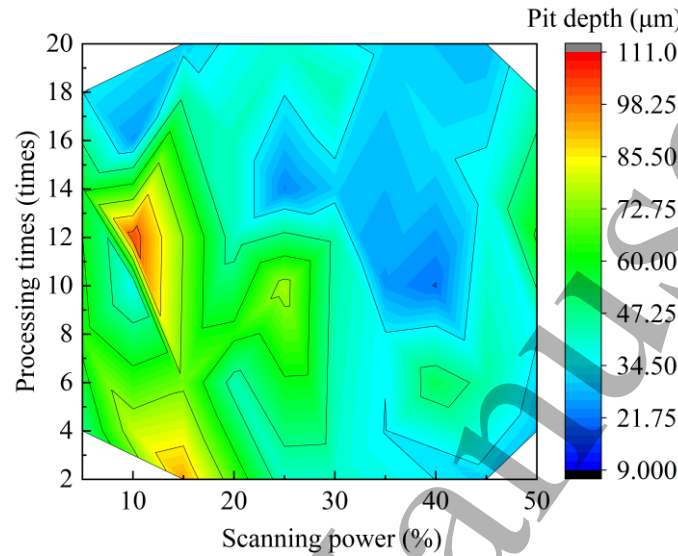


Figure 7. 2D contour map of the measured pit depth data

### 3.4 Analysis of depth fluctuation

The smaller the depth fluctuation, the smoother the pit bottom. The depth fluctuation ratio  $\Delta H$  (the ratio of depth fluctuation to pit depth) was analyzed. First, a correlation analysis between depth fluctuation and processing parameters was conducted, as shown in Table 10.

Table 10. Correlation analysis of the depth fluctuation rate and processing parameters

Correlation		Laser power ( $P$ )	Scanning speed ( $V$ )	Laser frequency ( $F$ )	Scanning times ( $N$ )
Depth fluctuation ( $\Delta H$ )	Pearson correlation	-.039	-.040	-.145	-.042
	Significance (Two-tailed)	.811	.807	.372	.799

\*\*Indicates that the correlation is significant at a confidence level (two-tailed) of 0.01.

\*Indicates that the correlation is significant at a confidence level (two-tailed) of 0.05.

The correlation analysis shows that there is no significant correlation between depth fluctuation and processing parameters for this batch of experiments, so regression analysis cannot be applied. However, depth fluctuation is an important criterion for evaluating the quality of surface textures. Therefore, a 2D contour map of the measured data was created, as shown in Figure 8. The plot indicates that the smallest depth fluctuation occurs within the laser power range of 10% to 20% and scanning times between 8 and

18. In addition, comparing the statistical analysis of depth fluctuation and pit depth, it is found that laser power and scanning times have the same influence on the results of both. For specific reason analysis, please refer to “3.3 Regression analysis of pit depth”.

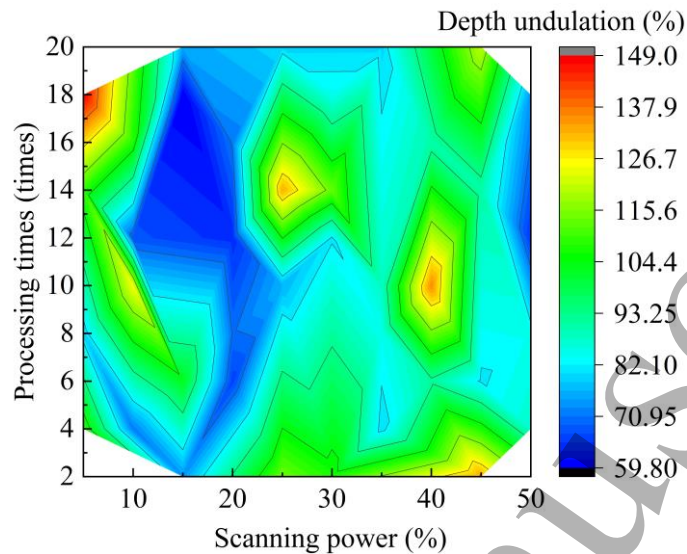


Figure 8. 2D contour map of the measured depth fluctuation rate data

#### 4. Conclusions

This study investigated laser surface texturing for finger seals. To evaluate the machining quality, four morphological parameters were established. Using uniform experiments and regression analysis methods, the influence of laser processing parameters on processing quality and their synergistic effects were analyzed, laying the foundation for friction and wear tests of textured finger seals. The main conclusions are as follows:

(1) The processing parameters that significantly affect the laser surface texturing for finger seals are the laser power, scanning times, and scanning speed.

(2) The outer diameter is directly proportional to the laser power and inversely proportional to the scanning speed. The bottom diameter ratio is directly proportional to the laser power and scanning times. The pit depth and depth fluctuation increase initially and then decrease with increasing laser power and scanning times.

(3) The suitable range of laser processing parameters is as follows: laser power (10~20%), scanning speed (400~700 mm/s), scanning times (8~18), and laser frequency (20~25 kHz).

#### Declaration of Conflicting Interests

The author(s) declared no potential conflicts of interest concerning the research, authorship, and/or publication of this article.

## Acknowledgements

The author(s) would like to thank the support from the National Natural Science Foundation of China (Grant No.52075436), the Department of Education in Hunan Province (Grant No. 23C0249), and the New Energy Vehicle Research Center at Hunan Institute of Engineering.

## References

- [1] Yin M-H, Zhang Y-C, Zhou R-M, Zhai Z-Y, Wang J-L, Cui Y-H, Li D-S. Friction Mechanism and Application of PTFE Coating in Finger Seals[J]. Tribology Transactions, 2022, 65(2): 260-269.
- [2] Wang Q, Zhang F, Huang Q, Ji H. Rapid evaluation method for radial critical operating capacity of finger seal[J]. Journal of Propulsion Technology, 2024, 45(7).
- [3] Lu F, Lu L, Liu J, Pang X, Song C. Tribological Properties and Wear Mechanism of C/C Composite Applied in Finger Seal[J]. Machines, 2023, 11(2).
- [4] Du C, Wang Y, Zhang Y, Song D, Ji H. An mathematical calculation method for radial limit deformation of arc-shaped finger seal[J]. Journal of Propulsion Technology, 2024, 45(7).
- [5] Wang J, Zhang Y, Hu H, Ji Y, Li J, Cui Y. Stress Field Evolution of Antifriction Wear-Resistant Sealing Coatings on GH4169 Superalloy Substrate under Thermal Shock[J]. Journal of Materials Engineering and Performance, 2024.
- [6] Wang Y T, Ke C J, Wu T H, Zhao X R, Wang R. Nanosecond laser texturing with hexagonal honeycomb micro-structure on Titanium for improved wettability and optical properties[J]. Optik, 2019, 192: 9.
- [7] Kumar C S, Patel S K. Effect of WEDM surface texturing on Al<sub>2</sub>O<sub>3</sub>/TiCN composite ceramic tools in dry cutting of hardened steel[J]. Ceramics International, 2018, 44(2): 2510-2523.
- [8] Grützmacher P G, Profito F J, Rosenkranz A. Multi-Scale Surface Texturing in Tribology-Current Knowledge and Future Perspectives[J]. Lubricants, 2019, 7(11): 42.
- [9] Wos S, Koszela W, Pawlus P, Drabik J, Rogos E. Effects of surface texturing and kind of lubricant on the coefficient of friction at ambient and elevated temperatures[J]. Tribology International, 2018, 117: 174-179.
- [10] Wang W, Zhao W H, Guo P Z, Liu Q, Kouediatouka A N, Dong G N. A textured surface with oil inflow and outflow function designed for starved lubrication[J]. Tribology International, 2023, 184: 8.
- [11] Zhou D, Xu Y, Gao X, Huang H H, Lv S J. Experimental Study on the Reduction Effect of Pit Texture on Disassembly Damage for Interference Fit[J]. Chinese Journal of Mechanical Engineering, 2023, 36(1): 12.
- [12] Velayuthaperumal S, Radhakrishnan R. Effect of different laser texture configurations on improving surface wettability and wear characteristics of Ti6Al4V implant material[J]. Journal of the Brazilian Society of Mechanical Sciences and Engineering, 2023, 45(7): 14.
- [13] Chen L, Zhang Y, Cui Y, Wang J, Wang M. Effect of snake-biomimetic surface texture on finger sealing performance under hydrodynamic lubrication[J]. Surface Topography-Metrology and Properties, 2021, 9(3): 1-14.
- [14] Chen L, Zhang Y, Cui Y, Wang J, Wang M. Effects of Snake-Bioinspired Surface Texture on the Finger-Sealing Performance under Varied Working Conditions[J]. Machines, 2022, 10(7): 1-20.
- [15] Koo S J, Kim H S. The homogeneity of multi-textured micro-pattern arrays in a laser shock surface patterning process and its effect on the surface properties of aluminum alloy[J]. Surface & Coatings Technology, 2020, 382: 1-13.
- [16] Dashtbozorg B, Li X, Romano J-M, Garcia-Giron A, Sammons R L, Dimov S, Dong H. A study on the effect of ultrashort pulsed laser texturing on the microstructure and properties of metastable S phase layer formed on AISI 316L surfaces[J]. Applied Surface Science, 2020, 511: 1-13.
- [17] Zhou C, Wu X, Lu Y, Wu W, Zhao H, Li L. Fabrication of hydrophobic Ti<sub>3</sub>SiC<sub>2</sub> surface with micro-grooved structures by wire electrical discharge machining[J]. Ceramics International, 2018, 44(15): 18227-18234.

- [18] Bae W-G, Kim D, Song K Y, Jeong H E, Chu C N. Engineering stainless steel surface via wire electrical discharge machining for controlling the wettability[J]. *Surface & Coatings Technology*, 2015, 275: 316-323.
- [19] Maharana H S, Kumar R, Murty S, Ramkumar J, Mondal K. Surface micro-texturing of dual phase steel and copper by combining laser machining and electrochemical dissolution[J]. *Journal of Materials Processing Technology*, 2019, 273: 1-13.
- [20] Koyano T, Hosokawa A, Takahashi T, Ueda T. One-process surface texturing of a large area by electrochemical machining with short voltage pulses[J]. *Cirp Annals-Manufacturing Technology*, 2019, 68(1): 181-184.
- [21] Shi L P, Fang Y, Dai Q W, Huang W, Wang X L. Surface texturing on SiC by multiphase jet machining with microdiamond abrasives[J]. *Materials and Manufacturing Processes*, 2018, 33(13): 1415-1421.
- [22] Xing Y, Luo C, Wan Y, Huang P, Wu Z, Zhang K. Formation of bionic surface textures composed by micro-channels using nanosecond laser on Si<sub>3</sub>N<sub>4</sub>-based ceramics[J]. *Ceramics International*, 2021, 47(9): 12768-12779.
- [23] Li F R, Li C, Zhou J, He J T, Wang J B, Luo C, Li S. Effect of Laser Parameters on Surface Texture of Polyformaldehyde and Parameter Optimization[J]. *Strojnicki Vestnik-Journal of Mechanical Engineering*, 2024, 70(5-6): 247-258.
- [24] L Y, Y D, B C, J H, G W, Y W. Investigations on femtosecond laser modified micro-textured surface with anti-friction property on bearing steel GCr15[J]. *APPLIED SURFACE SCIENCE*, 2017, 434: 12.
- [25] J A-T, M A, W P, J D D. Influence of laser parameters in surface texturing of Ti6Al4V and AA2024-T3 alloys[J]. *Opt Lasers Eng*, 2018, 103: 9.
- [26] Wu X Z, Zhou W B, Kodera Y, Garay J E. Nonlinear optical effects in polycrystalline transparent Al<sub>2</sub>O<sub>3</sub> ceramics using femtosecond laser pulses-supercontinuum generation and laser damage[J]. *Applied Physics Letters*, 2024, 124(10): 7.
- [27] Aguilar-Morales A I, Alamri S, Kunze T, Lasagni A F. Influence of processing parameters on surface texture homogeneity using Direct Laser Interference Patterning[J]. *Optics and Laser Technology*, 2018, 107: 216-227.
- [28] Madapana D, Bathe R, Manna I, Majumdar J D. Laser surface structuring of titanium alloy (Ti-6Al-4V) for improved tribocorrosion resistance for bio-implant applications[J]. *Tribology International*, 2024.
- [29] Shi Z, Duan X F, Chen Z H, Liu B, Fu H, Ji J H, Zhang Y H. Precision fabrication of micro-textures array for surface functionalization using picosecond pulse laser[J]. *Optics and Laser Technology*, 2024, 177: 14.
- [30] Fan Y, Li B, Lu J, Xia J, Liu F, Qiu X. Study on Morphology Evolution of GCr15 Steel by Nanosecond Laser Ablation[J]. *Chinese Journal of Lasers*, 2023, 50(20).
- [31] Xiao G, Liu S, He Y, Liu G, Zhu S, Song S. Defocus control and surface topography of titanium alloy laser belt processing[J]. *Acta Aeronautica et Astronautica Sinica*, 2022, 43(4).
- [32] Datta S, Raza M S, Muvvala G, Saha P, Pratihari D K. The effect of different laser head angles and shielding gas supply systems to maximize the depth of penetration by minimizing the plasma shielding effect in fiber laser welding of 3-mm thick NiTiInol sheet[J]. *Optik*, 2023, 283: 14.

## Appendix

**Table A1. Application scope, advantages and disadvantages of common texture processing technologies**

Processing technology	Scope of application	Advantage	Shortcoming
Laser surface texturing (LST)	Suitable for almost all materials	Wide range of applicable materials, wide processing scale, high processing efficiency	More expensive equipment

<b>Processing technology</b>	<b>Scope of application</b>	<b>Advantage</b>	<b>Shortcoming</b>
Electric discharge machining (EDM)	Suitable for conductive materials	The processing cost is low, and the processing of small-scale microtexture has high precision	Low material removal rate, not suitable for nonconductive materials
Wire electrical discharge machining (WEDM)	Suitable for most materials	High material removal rate and good processing quality	The processing cost is high and only grooves can be processed
Electrolytic machining (ECM)	Suitable for metal materials	High machining accuracy, small deformation, and the size of the workpiece is not limited	The need to replace electrodes or make masks leads to low processing efficiency and high cost
Abrasive jet machining	Suitable for gears, pistons, etc.	Simple operation and high efficiency	Machining accuracy is difficult to control
Traditional processing technology	Suitable for hard and brittle materials	High-machining precision and low cost	Poor machining stability
Chemically reactive ion etching	Suitable for most materials	High processing efficiency	Environmental pollution, high equipment maintenance costs
Photoetching	Semiconductor	High machining precision	Expensive equipment
3D printing	Metals, ceramics, and other materials with complex structures	High machining precision, good surface quality	Low processing efficiency, high cost, difficulty in mass production
Nanoimprint	Suitable for almost all materials	High machining precision, good surface quality, easy mass production	Expensive equipment

Accepted Manuscript